Virology 484 (2015) 194–202

Contents lists available at ScienceDirect

Virology

journal homepage: www.elsevier.com/locate/yviro

Three cardiovirus Leader proteins equivalently inhibit four different nucleocytoplasmic trafficking pathways

Jessica J. Ciomperlik [a], Holly A. Basta [b], Ann C. Palmenberg [a,*]

[a] Institute for Molecular Virology, and Department of Biochemistry, University of Wisconsin-Madison, Madison, WI, United States
[b] Department of Biology, Rocky Mountain College, Billings, MT, United States

ARTICLE INFO

Article history:
Received 20 April 2015
Returned to author for revisions
7 May 2015
Accepted 4 June 2015
Available online 23 June 2015

Keywords:
Nucleocytoplasmic trafficking inhibition
Cardiovirus
Leader protein
Okadaic acid

ABSTRACT

Cardiovirus infections inhibit nucleocytoplasmic trafficking by Leader protein-induced phosphorylation of Phe/Gly-containing nucleoporins (Nups). Recombinant Leader from encephalomyocarditis virus, Theiler's murine encephalomyelitis virus and Saffold virus target the same subset of Nups, including Nup62 and Nup98, but not Nup50. Reporter cell lines with fluorescence mCherry markers for M9, RS and classical SV40 import pathways, as well as the Crm1-mediated export pathway, all responded to transfection with the full panel of Leader proteins, showing consequent cessation of path-specific active import/export. For this to happen, the Nups had to be presented in the context of intact nuclear pores and exposed to cytoplasmic extracts. The Leader phosphorylation cascade was not effective against recombinant Nup proteins. The findings support a model of Leader-dependent Nup phosphorylation with the purpose of disrupting Nup-transportin interactions.

Introduction

Cardioviruses, as members of the *Picornaviridae* family, are positive-sense, single-stranded RNA viruses. Their preferred hosts are rodents, although some will readily infect other mammals. Of the three recognized species in this genus, two are represented by encephalomyocarditis virus (EMCV) and Theiler's murine encephalomyelitis virus (TMEV). Saffold virus (SafV), within the same Cardiovirus B species as TMEV, is one of the few members of this genus to infect humans (Jones et al., 2007). While cardioviruses have similar polyprotein organizations, each encodes a variable-length Leader (L) protein, none of which have homologs or analogs in other viruses or cells. Leader proteins are unique determinants of cardiovirus anti-host activities. Although not kinases themselves, the Leaders induce intense hyper-phosphorylation of certain Phe/Gly-containing nuclear pore proteins (Nups), including Nup62, Nup153 and Nup214 shortly after infection (Bardina et al., 2009; Porter and Palmenberg, 2009). Phosphorylation of Nups within nuclear pore complexes (NPC) down-regulates active nuclear import by hindering importin association with the Nups (Kehlenbach and Gerace, 2000; Kosako et al., 2009). This novel mechanism can be recapitulated by transfection of L-encoding cDNAs into cells or by the addition of recombinant L protein into cell extracts containing nuclei as targets (Porter and Palmenberg, 2009; Basta et al., 2014). The in vitro assays directly mimic the trafficking inhibition observed by cardiovirus infection-directed Nup phosphorylation.

The EMCV L (L_E) is 67 amino acids (aa) long. The NMR solution structure for the closely related Mengo L (L_M) shows an unusual N-proximal zinc-finger domain. The rest of the protein configures as random coil (Bacot-Davis et al., 2014). Functionally, the L_M coiled region has a C-proximal acid-rich domain and a central hinge segment which forms the primary induced-fit binding contacts with RanGTPase, a requisite partner in the anti-host activity (Porter et al., 2006; Bacot-Davis and Palmenberg, 2013; Basta and Palmenberg, 2014). L_E is shuttled to the nucleus after its polyprotein synthesis presumably by interactions with the viral 2A protein with which it can also interact (Petty et al., 2014). In the presence of guanine nucleotide exchange factor, RCC1, just inside the nuclear rim, L_E then exchanges 2A for Ran (Petty et al., 2014). The L_E interaction with this key trafficking regulator is very tight, with a measured K_D of about 3 nM (Petty and Palmenberg, 2013). Before, or shortly after this nuclear exchange, L_E becomes phosphorylated at Thr_{47} and Tyr_{41}, in steps which are obligating for the consequent L_E-dependent Nup phosphorylation activities (Basta et al., 2014). The NMR orientation of L_M, when bound to Ran, shows the pairing forces Ran into an allosteric conformation which mimics the RanGTP-bound active state of this transport regulator. As such, Ran (with L_M) becomes competent to bind exportins and

* Correspondence to: Ann C. Palmenberg. Institute for Molecular Virology, Robert M. Bock Laboratories, University of Wisconsin – Madison, 1525 Linden Dr., Madison, WI 53706. Fax: +1 608 262 6690.
E-mail address: acpalmen@wisc.edu (A.C. Palmenberg).

http://dx.doi.org/10.1016/j.virol.2015.06.004
0042-6822/

their cargos for putative shuttling to the cytoplasm (Bacot-Davis et al., 2014). It has been proposed that this complex (L_M:Ran: exportin), formed in the nucleus, subsequently recruits activated kinase cargos, such as p38 and/or ERK1/2 (Porter et al., 2010), and the full unit, unable to dissociate because of the bound Leader, becomes trapped in the nuclear pore, where the kinases catalyze the cell-debilitating hyper-phosphorylation of Nup62, Nup153 and Nup214 (Bacot-Davis et al., 2014).

The L proteins of SafV (L_S) and TMEV (L_T) are similar in many respects. Cardiovirus B species Leaders are 4 (L_S) to 9 (L_T) aa longer than L_E or L_M, with the added length mostly evident as short contiguous insertions C-terminal to the Ran-contact hinge domain. Each also has an additional small relative deletion next to the N-terminal initiating Met. Like L_M/L_E, the TMEV and SafV proteins become dually phosphorylated in cells or in recombinant form, but at different sites (i.e. Ser_{57} and Thr_{58}, respectively) and by different kinases (AMPK, not CK2) than the better studied EMCV systems (Basta and Palmenberg, 2014). When recombinant L_T or L_S, are introduced into cells, even in the absence of infection, they can indeed induce Nup62 phosphorylation, the common assay for hyper-phosphorylation (Basta et al., 2014).

There are many elements of the L-directed Nup phosphorylation model that are not well understood. It is unknown, for example, if there are other Nup proteins which are targets (or non-targets) of the activated kinase complexes. The matrix protein of vesicular stomatitis virus (VSV) causes nucleocytoplasmic trafficking inhibition (Her et al., 1997) by complexing with Nup98 and the exportin Rae1 (Faria et al., 2005). Similar to a phenotype described for TMEV infections, where Nup98 is also reported to be phosphorylated (Ricour et al., 2009), VSV inhibition of Nup98-dependent trafficking stops the export of cellular mRNAs and prevents the transcription of interferon and chemokine products (Porter and Palmenberg, 2009; Le Sage and Mouland, 2013; Lidsky et al., 2006; Ricour et al., 2009). The full collection of Nup62, Nup98, Nup153 and Nup214 are also among the demonstrated substrates for human rhinovirus (RV) protease 2A. These cousins of the cardioviruses inactivate NPC import/export by multiple Nup cleavage reactions rather than by phosphorylation cascades (Gustin and Sarnow, 2002; Watters and Palmenberg, 2011). The sequence differences in specific $2A^{pro}$ which are characteristic of the multiple RV genotypes allow individual viruses to preferentially cleave selected cohorts of Nup substrate panels with different avidities and rates (Watters and Palmenberg, 2011). Consequently, not all import/export pathways are equivalently disabled by every RV, allowing each $2A^{pro}$ sequence to manifest as a strain-specific Nup degradation pattern (Watters et al., under review).

With the cardioviruses, it is not known whether L_E-directed Nup hyper-phosphorylation is aimed more generically at all transport pathways, or like the RV, is more selectively directed at only those import/export units which use particular subsets of Nups. Cardiovirus systems to test these parameters have typically linked traceable reporters (e.g. GFP) to peptide fragments (e.g. SV40) with non-specific nuclear import localization signals (NLS), or tried to follow common cellular mRNAs as the metric for nuclear egress (Porter et al., 2006). These previous experiments are less sensitive than the newer, path-specific assays recently described for the RV (Watters et al., under review). Application of those new systems now provides clarification on the scope of L_X disruption of trafficking pathways for the L_E, L_S and L_T proteins, and as described here, show all 3 of these viruses act ubiquitously against 4 tested pathways, including a path dependent upon a nuclear export signal (NES) for protein egress. Moreover, observation of L_X-dependent Nup phosphorylation becomes accelerated in cell-free systems by the presence of okadaic acid (OA), an inhibitor which prevents counterproductive phosphatase activities on both the susceptible Nups and on the required cellular kinases.

Results

Nup98 and Nup50

Transfection of cells with L_X-encoding cDNAs, followed by Western analyses is the standard assay for L_X-dependent Nup phosphorylation (Porter et al., 2006). Some prior experiments also

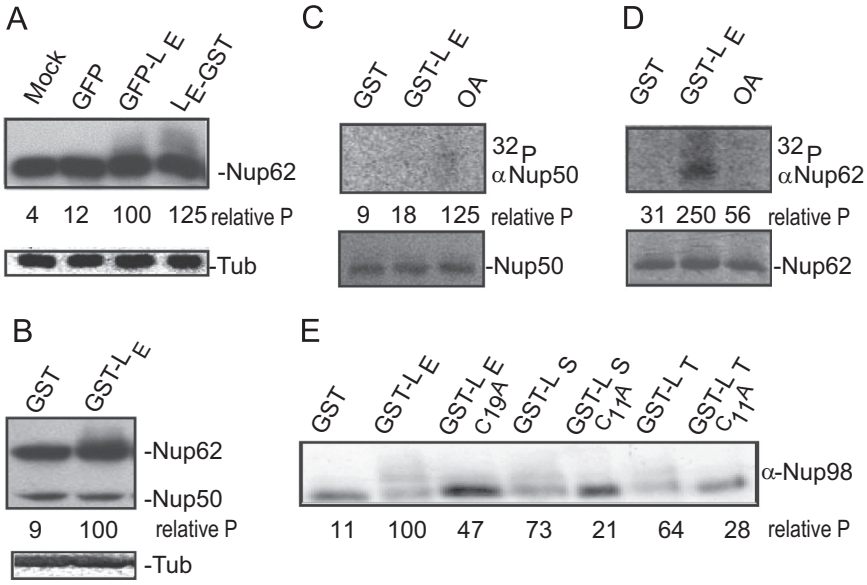

Fig. 1. Nup phosphorylation assays. (A) HeLa cells were transfected with cDNAs encoding the indicated proteins. After 16 h, harvested lysates were probed in Western assays using mAb414 (Nup62) or α-tubulin (Tub). (B) Recombinant L_E-GST or GST-L_E proteins (5 μg) were incubated with HeLa cytosol supplemented with isolated nuclei. After 45 min, the samples were fractionated, then probed by Western analyses as in A. (C) HeLa nuclei, cytosol and recombinant GST or GST-L_E were incubated with $\gamma^{32}P$ –ATP in the presence or absence of okadaic acid (OA). After incubation at 37 °C for 45 min, proteins reactive with α-Nup50 were extracted and fractionated. Upper panel is an autoradiogram. Lower panel is a silver stain of the same materials. (D) Same as C, except immunoprecipitation was with α-Nup62. (E) Similar to A, unlabeled transfected lysates were fractionated, then probed in Western assays with α-Nup98. In panels A, B, E, the "relative P" is pixel count (TotalLab software) in the phosphorylated product, normalized to GFP-L_E or GST-L_E controls. For C, D, these values are the relative pixels in the labeled bands, normalized to the silver stain signals.

evaluated Westerns or γ^{32}P incorporation after incubation of recombinant L_X proteins with fractionated cell nuclei and cytosol (Bacot-Davis and Palmenberg, 2013). The size (67–76 aa) and charge (pI ~3) of L_X proteins presents technical issues unless these segments are linked to fusion tags, such as GST or GFP (Porter et al., 2010). For L_E, the observed Nup phosphorylation after cDNA transfection was comparably strong (Basta et al., 2014) whether the tag was N-terminal (e.g. GFP-L_E), or C-terminal (e.g. L_E-GST), as illustrated in Fig. 1A. The common detection antibody (mAb414) recognizes multiple Phe/Gly-containing Nups, albeit with differing affinities. Typically, Nup62 modifications manifest on gels as a "smear" towards higher mobility when multiple phosphates are added sequentially. The change is distinctive whether L_E is assayed after transfection of cDNA (e.g. Fig. 1A), or as recombinant protein in cell-free extracts (e.g. Fig. 1B). The same is true for Nup153 and Nup214 (Porter and Palmenberg, 2009). Nup50 and Nup98, however, are only intermittently detectable with this mAb (e.g. Fig. 1B). For these, evaluation of the L_X-dependent changes required different reagents. Cytosol/nuclei mixtures similar to Fig. 1B, were labeled with γ^{32}P –ATP, and then extracted with mAbs specific to Nup50 or Nup62. While Nup50 was observable by Western analysis (Fig. 1B), the presence of GST-L_E, did not direct detectable label incorporation (Fig. 1C), nor did it shift in molecular weight. Nup62 on the other hand, was demonstrably labeled with ^{32}P by the inclusion of GST-L (Fig. 1D). Equivalent Nup98 reagents are not effective in similar immunoprecipitation experiments. For this evaluation, HeLa cells were transfected with cDNAs encoding L_E-GST, L_S-GST, L_T-GST, and also with corresponding cognates encoding Cys-to-Ala L_X-inactivating mutations (Basta et al., 2014). In every case when there was active L_X protein, the Nup98 mAb detected the upward "smear" of L_X-dependent phosphorylation. The activities ranked as $L_E > L_S > L_T$ for these particular conditions. Therefore, Nup98 but not Nup50, is a target of the L_E-dependent phosphorylation cascades (Fig. 1E).

Import/export pathway imaging

During EMCV infections, L_X cDNA transfections, or cell-free reactions with recombinant proteins, NPC active import/export is abrogated. Small proteins (< 40 kD) and metabolites then diffuse across the NPC to equilibrium (Porter and Palmenberg, 2009). Visualization of this process requires addition of fluorescent reporters linked to NLS sequences to record relative changes in nuclear/cytoplasmic cellular distribution. Recombinant GST-GFP_{NLS}, for example, was previously tracked in digitonin-treated HeLa cells to document GST-L_E concentration and rate effects (Porter and Palmenberg, 2009). HT_{NLS} (Halotag), transfected as cDNA into cells, showed similar relocalization (Bardina et al., 2009; Porter and Palmenberg, 2009; Lidsky et al., 2006). In all these previous experiments however, the tested reporter-NLS was from SV40, which traffics via the importin α/β pathways and is responsive only to particular segments of the Nup cohort (Table 1) specific to that karyopherin passage through the NPC (Fagerlund et al., 2005; Kumar et al., 2000; McBride et al., 2002).

The impact of L_X on other characterized transport pathways was assessed with HeLa cell lines transduced with mCherry reporter genes (~30 kD) linked to additional NLS/NES segments (~15–45 aa; (Watters et al., under review)). After infection with vEC_9 (3 h), the cells and controls were fixed, stained with DAPI and imaged (Fig. 2). Averaged pixel scans centered over the width of individual nuclei showed that the mCherry signals, compared to steady-state DAPI, diminished measurably after infection of cells, if the reporter was linked to the SV40 NLS, the M9 NLS (Pollard et al., 1996), or the RS domain NLS from an SR protein, splicing factor 2 (Kataoka et al., 1999). Previous characterization of these cells with rhinovirus reagents confirmed the cell-wide stability of the total mCherry signal (Watters et al., under review). The reporter signal redistributes out of nuclei during infection, but is not degraded. The fourth tested cell line expressed mCherry linked to the leucine-rich NES from PKI (Wen et al., 1995). This segment is sensitive to Crm1-mediated active nuclear egress. Here, the initial nuclear exclusion of the reporter was reversed after infection, allowing a stronger mCherry signal to accumulate in the nuclei relative to control cells. For each of these 4 lines, infection with vEC_9 impacted the respective mCherry-labeled NPC transport pathway. Virus disruption of active transport into or out of the nuclei resulted in reporter redistribution by diffusion relative to the steady-state DAPI signals.

The L_E protein of intact vEC_9 is the effector for the experimental set depicted in Fig. 2. Cell visualization assays with the same mCherry cell lines were repeated after transfection with cDNAs encoding L_E-GST, L_T-GST or L_S-GST. Again, averaged pixel scans centering on the nuclei illustrated the impact of L_X on mCherry relocalization (Fig. 3), this time in live, unfixed cells. Within these graphs, the solid lines now represent the mCherry profiles observed in control cells (i.e. equivalent to Fig. 2, mock). Relative to this, expression of all three L_X proteins mediated measurable reporter diffusion out of (NLS lines), or into (NES line) nuclei. Unlike the rhinovirus $2A^{pro}$ which can discriminate these respective import/export systems according to virus genotype (Watters et al., under review), the 3 cardiovirus L_X proteins seemed equivalently adept at disrupting all 4 tested transport pathways (Fig. 3).

Context for Nup phosphorylation

L_X-dependent Nup phosphorylation assays typically present the substrates in the context of intact NPC, either by testing within whole cells (transfection, infection), or by reconstituting isolated cytoplasm and nuclei in the presence of recombinant protein (Porter and Palmenberg, 2009; Porter et al., 2010). The current hypothesis predicts that Ran-bound L_X, complexed with an exportin and activated kinase cargo, becomes trapped within an NPC, leading to Nup hyperphosphorylation (Bacot-Davis et al., 2014). Recombinant GST-Nup62 (Watters and Palmenberg, 2011) and His-Nup98 (personal communications, K.E. Watters) have been demonstrated as native-like substrates for RV $2A^{pro}$. But when either protein was added to sonicated HeLa cell whole-cell extracts, or to subcellular fractionated HeLa cytosol, GST-L_E failed to induce detectable phosphorylation (Fig. 4A and B). The whole-cell lysates and HeLa cytosol each contain endogenous Nups, either as precursors to nascent NPC assembly (cytosol), or from the cell disruption (whole cell lysates). For Nup62 the native and recombinant forms are easy to distinguish by size (Fig. 4B). For Nup98, the proteins co-migrate, but rNup98 phosphorylation would still be evident by measuring the A/B area ratios on the Western blot as detected with the His-tag mAb (Fig. 4A). Although all these samples also contain Ran, Crm1, and kinases, in the absence of intact nuclei, neither the recombinant nor the endogenous Nups became phosphorylated in an L_E-dependent manner. It requires the addition of intact nuclei back to these mixtures to see evidence of Nup phosphorylation. Even then, however, recombinant proteins were still not viable substrates. The Nup phosphorylation mechanism was capable of discriminating context and modified only the native Nups, presumably those presented by the nuclei NPC.

Kinase activation

Inhibitor experiments have implicated mitogen-activated protein kinases (MAPK), particularly ERK1/2 and p38, as the probable pathways involved in Nup phosphorylation during EMCV

Table 1
Nups associated with NPC pathways.

NLS/NES Motif sequence	Required Nups[a]	Karyopherin[a]
Classical import pathway. NLS is from the SV40 large T-antigen protein	Nup62 Nup214 Nup98 Nup358 Nup153	importin α/β
M9-mediated import pathway. NLS is from the M9 domain of mRNA binding protein hnRNPA1	Nup62 Nup98 Nup153	transportin 1
RS-mediated import pathway. NLS is from the RS domain of splicing factor 2, an SR (Arg/Ser-rich) protein.	Nup98 Nup153	transportin 3
Leucine-rich NES-mediated export pathway. NES is from the protein kinase A inhibitor (PKI)	Nup62 Nup214 Nup98 Nup358 Nup153	Crm1

[a] Nup and karyopherins assignments are reviewed in Terry and Wente (2009); Ryan and Wente (2000).

infections or L_E-dependent cDNA transfections (Porter et al., 2010). In intact cells, activation of both enzymes can be observed in the presence of L_E, independent of the simultaneous activation of their upstream signaling cascades, including MEK1/2, MKK3, MKK6 and cRaf. The pathway activation points must then be at or near the effector enzymes themselves (Porter et al., 2010), potentially involving phosphatases rather than kinases as the regulatory mediators. This idea was tested with the reconstituted cytosol and nuclei mixes, supplemented with GST-L_E (Fig. 5). As described above, this experimental combination gives effective Nup hyperphosphorylation. Surprisingly though, only very weak signals were detected with mAbs specific to the phosphorylated effector kinases (Fig. 5AB, GST-L_E lanes). Reasoning that the activated kinases could be cycling, the protein phosphatase 1/2a inhibitor, okadaic acid (OA) was added at a concentration that inhibits such enzymes (Cohen et al., 1990). The OA increased the phosphorylated ERK1/2 and p38 signals by at least 10–20 fold, presumably by preventing dephosphorylation within the MAPK pathways and allowing the intermediates to accumulate (Ho et al., 1997). In the absence of GST-L_E, OA had only a modest effect on Nup62 phosphorylation in these reactions, as measured by autoradiography (Fig. 1D, OA lane). It is known that some Nups, including p150 in *Drosophila* cells, can become phosphorylated by CDK1 in the presence of OA (Onischenko et al., 2005), as are other non-specific Nups in mammalian cells (4). Nup50 contains a phosphatase-sensitive phosphorylation site (Kosako et al., 2009). Indeed, in the cell-free reconstitution assays this observation was confirmed by low-level incorporation of γ^{32}P into Nup50-specific material (Fig. 1C) in the presence of OA.

Discussion

ERK1/2 and p38 have been implicated as effector kinases in L_E-dependent Nup hyper-phosphorylation (Porter et al., 2010). In phosphor-proteomics studies (Kosako et al., 2009) Nup50 has been suggested as a potential substrate for ERK1/2, and it was therefore of interest to assay this protein's putative alterations in the presence of L_E. Although in the presence of the phosphatase inhibitor OA (without GST-L_E), Nup50 did become labeled with γ^{32}P, L_E did not direct this event (Fig. 1C). Under similar circumstances, in addition to the previously described phosphorylation of Nup62, Nup153 and Nup214, the phosphorylation of Nup98 was readily observed and dependent upon the presence of active L_E, L_T and/or L_S sequences. The Nup phosphorylation by L_E required the substrates to be presented in the context of intact nuclei, because when tested with parallel recombinant versions of Nup62 or Nup98 that do not become incorporated into nuclear pores, the L_E-dependent mechanism only altered the native proteins (Fig. 4). Though some substrate-altering aberration of the recombinant Nups cannot be entirely ruled out, proximity (possibly through trapping the L_X:Ran complexes within the NPC) is the most likely explanation for this observed mechanistic preference. If captured within the NPC, limited catalytic amounts of the L_X complexes might then direct massive hyperphosphorylation of the preferred substrates.

When rhinoviruses infect cells, the virus-encoded $2A^{pro}$ cleave many of the same subset of NPC Nups affected by L_X-dependent hyperphosphorylation (Gustin and Sarnow, 2002; Watters and Palmenberg, 2011). As it is with the cardioviruses, the effect is down regulation of active nuclear import/export and redistribution of diffusible proteins throughout the cell. A special characteristic of the rhinovirus system, though, is that not all import/export pathways are affected equivalently. The genotype-specific sequences of individual $2A^{pro}$ have different Nup cleavage preferences (Watters and Palmenberg, 2011), and therefore, the order, rate and location of each NPC cleavage can be used by these viruses to regulate the specific activities of nucleocytoplasmic cargo exchange. This has been demonstrated for the SV40, M9 and RS NLS-dependent import pathways and the Crm1-dependent export pathway (Watters et al., under review). The classical NLS (SV40) pathway uses karyopherins importin α/β to transport a broad range of cargos (Adam and Adam, 1994; Gorlich et al., 1995). After the cargo:karyopherin complex is formed, it traverses the NPC via transient interactions with preferred Phe/Gly sites on multiple Nups (see Table 1), including Nup62, Nup98, Nup153, Nup214 and Nup358 (Moroianu et al., 1995). The M9 nuclear localization signal is from the mRNA binding protein hnRNPA1. It is recognized by transportin1 (karyopherin B2 in yeast, reviewed in Cook et al. (2007), which is also responsible for import of HIV-1 Rev into the nucleus. The RS sequence from splicing factor 2 is recognized by transportin 3, a member of the karyopherin β family, and mediates the transport of SR proteins containing Arg-Ser-rich domains (RS) involved in the regulation of pre-mRNA splicing (Hedley et al., 1995; Lai et al., 2001). The PKI nuclear export pathway uses Crm1 (XPO1), a transportin which interacts with cargos or adapters bearing leucine-rich motifs (Fornerod et al., 1997) such as the HIV-1 Rev protein, the protein kinase A inhibitor (PKI), 5S rRNAs, and U snRNAs (Wen et al., 1995; Fischer et al., 1995).

It has been proposed that rhinoviruses, by subtly balancing the trafficking unique to these pathways, can tailor the cell's cytokine responses to needs of each genotype (Watters et al., under review). The cardiovirus L_X activities, however, when tested with these same pathways (Fig. 2 and 3) seemed to show an indiscriminant, brute force NPC attack mode. Although activated kinases frequently transit the NPC in their roles as transcription regulators (Zehorai et al., 2010), there are few reports of coincidental (or accidental?) Nup phosphorylation. In uninfected cells, some Nups do become partially phosphorylated during mitosis, contributing to the transient dissociation of the NPC, but the cardiovirus-fostered events are unique biological phenomena in the strength and extent of Nup targeting. Not only were all 4 tested import/export pathways compromised within 3 h of vEC_9 infection, but all

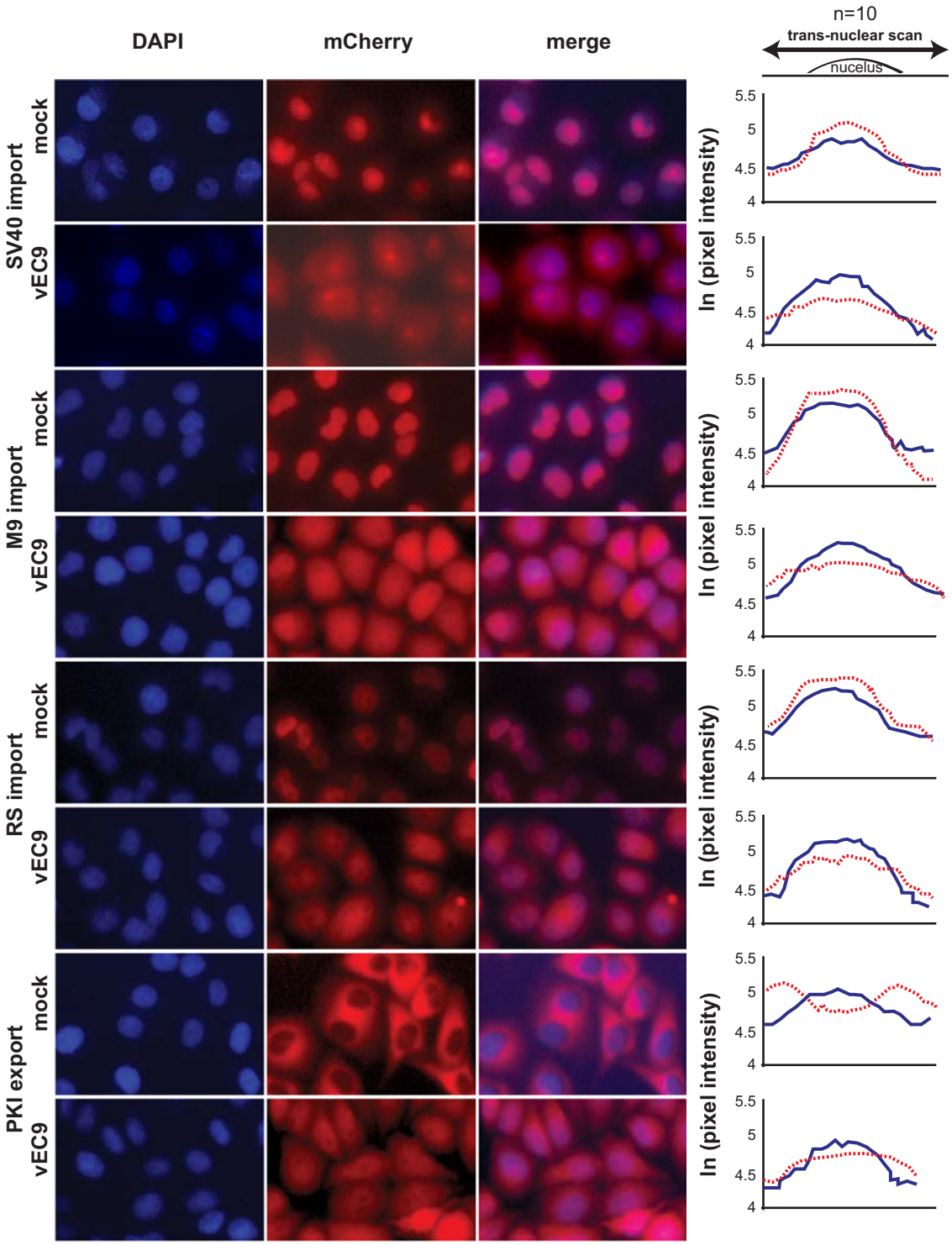

Fig. 2. Trafficking disruption by virus. Transduced HeLa cells expressing mCherry fusion proteins linked to NLS (SV40, M9 or RS) or NES (PKI) import/export sequences, were infected with vEC9 (MOI = 15). At 3 h, the cells were fixed, stained with DAPI and imaged. For each condition, randomly selected individual cells ($n = 10$) were scanned for pixel intensity (linear stretch of 80 pixels), centered on the DAPI signal. The values were averaged and plotted as the natural log of each signal for DAPI (blue solid line), and mCherry (dashed red line). The average standard deviation was 0.210 ln(x) (range: 0.124–0.274).

3 L_X-GST proteins, L_E, L_T and L_S, were equivalently effective against all of the pathways. Apparently, phosphorylation is a much less discerning method of NPC disruption than rhinoviruses' incisive proteolytic cleavage. The monitored processes also included measurable disruption of karyopherin-mediated NPC cargo export (i.e. Crm1). Although not directly tested here, one might expect the β3 importin 5 pathway, responsible for the transport of various ribosomal proteins, to be additionally hindered by L_X, as it requires the same subsets of altered Nups, including Nup62, Nup98, Nup153, Nup214 and Nup358 (Yaseen and Blobel, 1997; Jakel and Gurlich, 1998). Still, despite the obvious broad-based NPC changes brought about by hyper-phosphorylation, it was somewhat surprising to find a level of L_E-dependent substrate selection within these pores. Nup50, which is not phosphorylated by L_E, is also not implicated in any of the above transport pathways. This is despite observations that Nup50 can indeed, during normal cell cycling, be

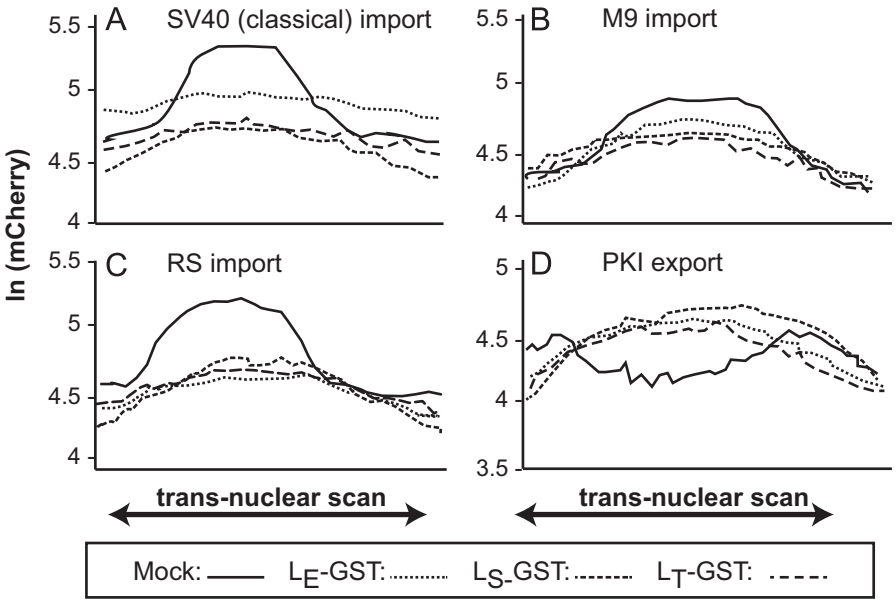

Fig. 3. Trafficking disruption by cDNAs. Similar to Fig. 2, transduced HeLa cells expressing mCherry fusion proteins linked to the SV40 NLS (A), M9 NLS (B), RS NLS (C) or PKI NES (D) were transfected with cDNAs for L_E-GST, L_S-GST or L_T-GST. After 16 h, individual live cells ($n=8$) were imaged for mCherry pixel intensity (linear stretch of 80 pixels) centered on the nucleus. Mock cells (solid lines) were transfected with cDNA for GST alone. The average standard deviation was 0.1274 ln(x) (range: 0.64–0.244).

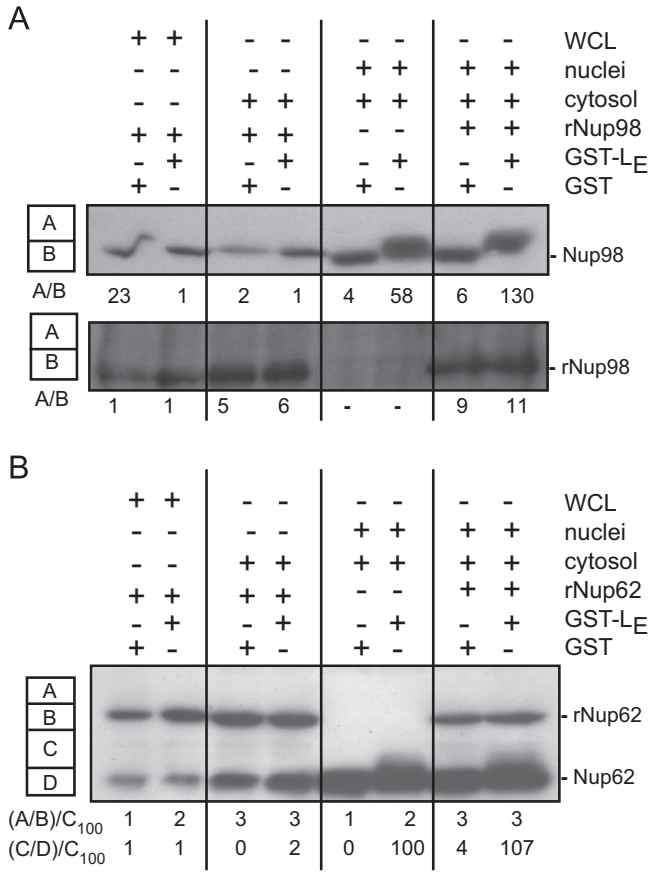

Fig. 4. Nup format. Cell-free systems containing HeLa whole-cell lysates (WCL), cytosol, or cytosol plus isolated nuclei, were reacted with recombinant GST or GST-L_E, in the presence or absence of recombinant His-Nup98 (A), or recombinant GST-Nup62 (B). After 45 min of incubation, the samples were fractionated, probed by Western analyses using α-Nup98 and α-His (A), or α-Nup62 (B). Pixel counts in the A, B, C, D boxes for each lane show the areas recorded and normalized to the control samples, as relative measures of observed phosphorylation.

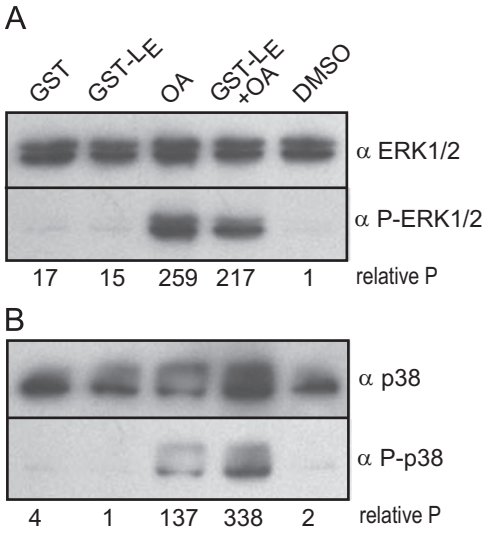

Fig. 5. Kinase activation. HeLa cytosol was reacted with recombinant GST or GST-L_E in the presence or absence of okadaic acid (OA) and/or DMSO. After 45 min of incubation, the samples were fractionated then probed by Western analyses using (A) α–ERK/12, α–P-ERK1/2, or (B), α-p38, α-P-p38. Pixel normalization for each lane was relative to the respective, unactivated forms (unphosphorylated) of the kinases.

phosphorylated by ERK1/2 (Kosako et al., 2009), among the enzymes implicated in the L_E mechanism (Porter et al., 2010). The potent phosphatase 1 and phosphatase 2a inhibitor OA, increased the pools of activated kinases, including ERK1/2 in the cell extracts, and allowed Nup50 phosphorylation. Phosphatases generally serve custodial roles during certain normal cellular events. In particular, protein phosphatases 1 and 2a interfere with MAPK pathways and are responsible for reversing any cyclin dependent kinase conferred- Nup phosphorylations acquired during mitosis (Onischenko et al., 2005). Full reconstitution of NPC during cell cycling actually requires this type of phosphate

curating, and these processes are therefore sensitive to OA (Onischenko et al., 2005).

Conclusions

Here, we present data that Nup hyper-phosphorylation pathways by L_E, L_T and L_S, all target Nup98, in addition to Nup62 (Porter and Palmenberg, 2009). Nup50, on the other hand was not phosphorylated by recombinant L_E protein, and by inference, during infection. Furthermore, L_E-dependent Nup phosphorylation in cell-free assays requires the substrates to be presented in the context of full nuclear pores (i.e. intact nuclei), as supplemented with cytosol (Porter et al., 2006). When this happens, at least 3 independent cellular importin pathways (importin α/β, transportin-1, transportin-3), and an exportin pathway (Crm1) become compromised, as monitored with cell lines transduced to express path-specific mCherry NLS/NES reporters.

Materials and methods

HeLa cell lines

Suspension cultures were maintained in modified Eagle's medium (37 °C, 10% calf serum, 2% FBS, under 5% CO_2). In addition to standard cells (ATCC CRL 1958), stable transduced cell lines carrying mCherry reporter genes linked to defined NLS/NES sequences have been described (Watters et al., under review). Briefly, the SV40 large T antigen NLS, M9 NLS (Pollard et al., 1996), the RS NLS from splicing factor 2 (Kataoka et al., 1999), or the leucine-rich NES from PKI (Wen et al., 1995) were engineered in-frame, C-terminal to an mCherry gene in the context of a retroviral vector plasmid encoding neomycin resistance (Sheehy et al., 2002). Moloney murine leukemia virus vectors were used in combination with these plasmids to create virus stocks harboring the respective genes. Infection of HeLa cells, genome integration and antibiotic selection gave cell lines with highly visible, constitutive expression of the mCherry derivatives. Before visualization, plated cells were rinsed with PBS (2 ×, 137 mM NaCl, 2.7 mM KCl, 10 mM Na_2HPO_4, pH 7.4), treated overnight at 4 °C with 4% paraformaldehyde, and then rinsed with PBS (3x) before the addition of DAPI (1 μg/ml).

Cell fractionation

HeLa cytosol was isolated after swelling suspension cells in hypotonic buffer (0.75 $Mg(OAc)_2$, 0.15 mM EDTA, 1 mM PMSF, 0.01 mg/ml leupeptin, 20 mM pepstatin A, 3 mM DTT), followed by dounce homogenization and clarification (16,000 × *g*, 20 min, 4 °C). TB (1/10 volume, 10 × at 20 mM hepes pH 7.3, 2 mM Mg $(OAc)_2$, 110 mM K(OAc), 1 mM EGTA) was added before storage at −80 °C. Whole cell lysates were prepared similarly, by the addition of WCLB (50 mM Tris pH7.4, 50 mM NaF, 5 mM $Na_4O_7P_2$, 1 mM EDTA, 1 mM EGTA, 250 mM mannitol, 1% triton × 100; 1 mM DTT, 1 mM PMSF, 20 mM pepstatin A, and 1 × protein phosphatase inhibitor cocktail 3, Sigma Aldrich) to cells, followed by sonication (2 ×, 30 s, 4 °C) and clarification (16,000 × *g*, 10 min). The materials were aliquoted and snap-frozen before storage at −80 °C. Nuclei were isolated from suspension cells following treatment with digitonin and clarification to remove cytosol (Mili et al., 2001). Briefly, the cells were collected, washed (2 ×, PBS), then incubated (10 min, 4 °C) in RSB (10 mM Tris–HCl, pH 7.4, 100 mM NaCl, 2.5 mM MgCl) with digitonin (40 μg/ml, Sigma Aldrich). The samples were clarified (2000 × *g*, 8 min), and the pellets were rinsed with RSB, then TB (plus 1 mM DTT, 3 ×). Quantitation was with a hemocytometer after staining with tryphan blue.

Transfection and infections

Eukaryotic expression plasmids for GST, GFP, GFP-L_E, L_E-GST, L_T–GST (BeAn), and L_S-GST (SafV-2) were as described (Basta and Palmenberg, 2014; Porter et al., 2010). The GST-L_X panel also had matched cognates encoding corresponding, inactive L_X sequences ($C_{19}A$, or $C_{11}A$). Cells were transfected (3×10^5 cells per well, 1 μg cDNA) using lipofectamine (1 μl, Invitrogen) in Opti-MEM media (Invitrogen), and then incubated (37 °C under 5% CO_2). Infections with vEC9 (Hahn and Palmenberg, 1995) used an MOI = 15, in PBS. At harvest, the wells were rinsed (2 ×, PBS) before 2 × SDS buffer was added. Cell materials were collected and boiled (15 min) before fractionation by SDS-PAGE and protein detection in Western assays.

Microscopy

Cells (live or fixed with paraformaldehyde) were visualized with a Ti–E ECLIPSE inverted wide-field microscope (Nikon Corporation). The images were collected using a CoolSnapHQ camera (Photometrics). Excitation/emission filter sets detected 460 nm (DAPI) and 632 nm (mCherry). Nikon NIS Elements software (version 4.30.01) was used to tabulate individual pixel intensities across an 80 pixel-window, centered on the nucleus, per cell. DAPI and mCherry data for a minimum of 8 live cells or 10 fixed cells per experimental condition were collected. The values were compiled in Excel and averaged across the 80 pixel windows. To compare conditions with fixed cells, the averaged DAPI levels were normalized. The natural log of each point in the intensity profile was plotted.

Recombinant proteins

Recombinant engineering, bacterial expression and protein isolation for GST and GST-L_E have been described (Porter et al., 2006). The isolation of recombinant GST-Nup62 (human) is also described (Watters and Palmenberg, 2011). Purified recombinant His-Nup98 (human) was a gift from Dr. Kelly Watters.

Westerns and antibodies

Samples were boiled with SDS buffer before the proteins were resolved by SDS-PAGE, and transferred to polyvinylidene difluoroide membranes (Immobilon-P, Millipore). The membranes were blocked (30 min) in TBST (20 mM Tris, pH 7.6, 150 mM NaCl, 0.5% Tween 20) with 10% dry milk as described (Porter and Palmenberg, 2009). For Western assays, the membranes were incubated with a primary antibody (in TBST, 1% dry milk, overnight, 4 °C), before rinsing (3 ×, TBST), and addition of a secondary antibody (1 h, 20 °C). After additional rinses (3 ×, TBST), the membranes were developed according to manufacturers' specifications for enhanced chemiluminescence (Pierce, GE Lifesciences). Antibodies included: α-Nup98 (goat mAb, IgG, Sigma, 1:10,000), α−FG-repeat Nups (murine mAb414, IgG, Covance, 1:2000), α-Nup62 (murine Ab, IgG, BD Transduction Laboratories, 1:2000), α-tubulin (murine Ab, IgG, Sigma, 1:10,000), α-Nup50 (goat Ab, Abcam, 1:2000), α–GST (murine mAb, IgG, Novagen, 1:10,000), α-His (6 × His, murine Ab, Abcam, 1:2000), α-P-p38 (activated, phospho-Thr180/Tyr182; rabbit Ab, IgG, Cell Signaling Technology, 1:3000), α−p38

(unactivated, rabbit Ab, IgG, Cell Signaling Technology, 1:3000), α–P-ERK1/2 (activated, phospho-Thr202/Tyr204 ERK 1/2; rabbit Ab, IgG, Cell Signaling Technology, 1:2000), α–ERK1/2 (unactivated, ERK1/2, rabbit Ab, IgG, Upstate, Millipore, 1:5000), α-mouse (secondary Ab, IgG, Sigma Aldrich, 1:8000), α-rabbit (secondary Ab, IgG, Promega, 1:8000) α-goat (secondary Ab, IgG, Sigma, 1:8000).

Nup50 and Nup62 immunoprecipitation

HeLa nuclei (10^6 cell equivalents) and fractionated cytosol (3×10^5 cell equivalents) were combined with γ-^{32}P –ATP (10 μCi). Recombinant GST or GST- L_E (2 μg), were added. Some samples were supplemented with okadaic acid (250 nM). Reactions were incubated at 37 °C for 45 min before the addition of RIPA (300 μl/sample, 50 mM Tris, pH 7.4, 150 mM NaCl, 0.1% SDS, 1% Triton ×100, 0.5% Na deoxycholate, 1 mM PMSF, 20 mM pepstatin A, and protein phosphatase inhibitor cocktail 3, Sigma Aldrich) and sonication. Protein G-conjugated beads (10 μl, G.E. Lifesciences) were added. Incubation was for 1 h before the beads were removed by centrifugation. Fresh protein-G beads conjugated to α-Nup50 or α-Nup62 (saturated) were incubated with agitation (4 °C, 3 h) and then collected. After extensive washing (6×, PBS with 0.02% triton), samples were denatured with SDS buffer, boiled and fractionated by SDS-PAGE. Protein bands were detected by silver-staining and autoradiography, with densitometry performed using a Typhoon imager (GE Healthcare).

Acknowledgments

The authors thank Drs. Nathan Sherer and Kelly Watters for microscopy assistance and the generation of mCherry cell lines, Jaye Gardiner for assistance with NIS Elements software, and Nathan Ciomperlik for assistance with data analysis. We thank Dr. Howard Lipton for the generous gift of SafV-2 and TMEV (BeAn) cDNAs, and Kelly Watters for the purified recombinant His-Nup98. This work was supported by NIH Grant AI017331 to ACP.

References

Adam, E.J.H., Adam, S.A., 1994. Identification of cytosolic factors required for nuclear location sequence-mediated binding to the nuclear envelope. J. Cell Biol. 125, 547–555.
Bacot-Davis, V.R., Palmenberg, A.C., 2013. Encephalomyocarditis virus Leader protein hinge domain is responsible for interactions with Ran GTPase. Virology 443, 177–185.
Bacot-Davis, V.R., Ciomperlik, J.J., Cornilescu, C.C., Basta, H.A., Palmenberg, A.C., 2014. Solution structures of Mengovirus leader protein, its phosphorylated derivatives, and in complex with RanGTPase. Proc. Natl. Acad. Sci. USA 111, 15792–15797.
Bardina, M.V., Lidsky, P., Sheval, E.V., Fominykh, K.V., van Kuppeveld, F.J., Polyakov, V.Y., Agol, V., 2009. Mengovirus-induced rearrangements of the nuclear pore complex: Hijacking cellular phosphorylation machinery. J.Virol. 83, 3150–3161.
Basta, H.A., Palmenberg, A.C., 2014. AMP-activated protein kinase phosphorylates EMCV, TMEV, and SafV Leader proteins at different sites. Virology 262, 236–240.
Basta, H.A., Bacot-Davis, V.R., Ciomperlik, J.J., Palmenberg, A.C., 2014. Encephalomyocarditis virus Leader is phosphorylated by CK2 and syk as a requirement for subsequent phosphorylation of cellular nucleoporins. J.Virol. 88, 2219–2226.
Cohen, P., Holmes, C.F.B., Tsukitani, Y., 1990. Okadaic acid: a new probe for the study of cellular regulation. Trends Biochem. Sci. 15, 92–102.
Cook, A., Bono, F., Jinek, M., Conti, E., 2007. Structural biology of nucleocytoplasmic transport. Annu. Rev. Biochem. 76, 647–671.
Fagerlund, R., Kinnuen, L., Kohler, M., Julkunen, I., Melen, K., 2005. NF-kappa B is transported into the nucleus by importin alpha3 and importin alpha4. J. Biol. Chem. 280, 15942–15951.
Faria, P.A., Chakraborty, P., Levay, A., Barber, G.N., Ezelle, H.J., Enninga, J., Arana, C., van Deursen, J., Fontoura, B.M., 2005. VSV disrupts the Rae1/mrnp41 mRNA nuclear export pathway. Mol. Cell 17, 93–102.
Fischer, U., Huber, J., Boelens, W.C., Mattaj, I.W., Luhrmann, R., 1995. The HIV-1 Rev activation domain is a nuclear export signal that accesses an export pathway used by specific cellular RNAs. Cell 82, 475–483.
Fornerod, M., Ohno, M., Yoshida, M., Mattaj, I.W., 1997. CRM1 is an export receptor for leucine rich nuclear export signals. Cell 90, 1051–1060.
Gorlich, D., Vogel, F., Mills, A.D., Hartmann, E., Laskey, R.A., 1995. Distinct functions for the two importin subunits in nuclear protein import. Nature 377, 246–248.
Gustin, K.E., Sarnow, P., 2002. Inhibition of nuclear import and alteration of nuclear pore complex composition by rhinovirus. J. Virol. 76, 8787–8796.
Hahn, H., Palmenberg, A.C., 1995. Encephalomyocarditis viruses with short poly (C) tracts are more virulent than their Mengo virus counterparts. J.Virol. 69, 2697–2699.
Hedley, M.L., Amrein, H., Maniatis, T., 1995. An amino acid sequence motif sufficient for subnuclear localization of an arginine/serine-rich splicing factor. Proc. Natl. Acad. Sci. USA 92, 11524–11528.
Her, L.-S., Lund, E., Dahlberg, J.E., 1997. Inhibition of Ran guanosine triphosphatase-dependent nuclear transport by the matrix protein of vesicular stomatitis virus. Science 276, 1845–1848.
Ho, D.T., Shayan, H., Murphy, T.H., 1997. Okadaic acid induces hyperphosphorylation of tau independently of mitogen-activated protein kinase activation. J. Neurochem. 68, 106–111.
Jakel, S., Gurlich, D., 1998. Importin β, transportin, RanBP5 and RanBP7 mediate nuclear import of ribosomal proteins in mammalian cells. EMBO 17, 4491–4502.
Jones, M.S., Lukashov, V.V., Ganac, R.D., Schnurr, D.P., 2007. Discovery of a novel human picornavirus in a stool sample from a pediatric patient presenting with fever of unknown origin. J. Clin. Microbiol. 45, 2144–2150.
Kataoka, N., Bachorik, J.L., Dreyfuss, G., 1999. Transportin-SR, a nuclear import receptor for SR proteins. J. Cell Biol. 145, 1145–1152.
Kehlenbach, R.H., Gerace, L., 2000. Phosphorylation of the nuclear transport machinery down-regulates nuclear protein import in vitro. J. Biol. Chem. 275, 17848–17856.
Kosako, H., Yamaguchi, N., Aranami, C., Ushiyama, M., Kose, S., Imamoto, N., Taniguchi, H., Nishida, E., Hattori, S., 2009. Phosphoproteomics reveals new ERK MAP kinase targets and links ERK to nucleoporin-mediated nuclear transport. Nat. Struct. Mol. Biol. 16, 1026–1035.
Kumar, K.P., McBride, K.M., Weaver, B.K., Dingwall, C., Reich, N.C., 2000. Regulated nuclear-cytoplasmic localization of interferon Regulatory Factor 3, a subunit of double stranded RNA-Activaed Factor 1. Mol. Cell Biol. 20, 4159–4168.
Lai, M.C., Lin, R.I., Tarn, W.Y., 2001. Transportin-SR2 mediates nuclear import of phosphorylated SR proteins. Proc. Natl. Acad. Sci. USA 98, 10154–10159.
Le Sage, V., Mouland, A.J., 2013. Viral subversion of the nuclear pore complex. Viruses 5, 2019–2042.
Lidsky, P.L., Hato, S., Bardina, M.V., Aminev, A.G., Palmenberg, A.C., Sheval, E.V., Polyakov, V.Y., van Kuppeveld, F.J., Agol, V., 2006. Nucleo-cytoplasmic traffic disorder induced by cardioviruses. J.Virol. 80, 2705–2717.
McBride, K.M., G. Banninger, M.C., Reich, N.C., 2002. Regulated nuclear import of the STAT1 transcription factor by direct binding of importin-alpha. EMBO 21, 1754–1763.
Mili, S., Shu, H.J., Zhao, Y., Pinol-Roma, S., 2001. Distinct RNP complexes of shuttling hnRNP proteins with pre-mRNA and mRNA: candidate intermediates in formation and export of mRNA. Mol. Cell Biol. 21, 7307–7319.
Moroianu, J., Hijikata, M., Blobel, G., Radu, A., 1995. Mammalian karyopherin alpha 1 beta and alpha 2 beta heterodimers; alpha 1 or alpha 2 subunit binds nuclear localization signal and beta subunit interacts with peptide repeat-containing nucleoporins. Proc. Natl. Acad. Sci. USA 92, 6532–6536.
Onischenko, E.A., Gubanova, N.V., Kiseleva, E.V., Hallberg, E., 2005. CDK1 and okadaic acid-sensitive phosphatases control assembly of nuclear pore complexes in drosophila embryos. Mol. Biol. Cell 16, 5152–5162.
Petty, R.V., Palmenberg, A.C., 2013. Guanine-nucleotide exchange factor RCC1 facilitates a tight binding between EMCV Leader and cellular Ran GTPase. J. Virol. 87, 6517–6520.
Petty, R.V., Basta, H.A., Bacot-Davis, V.R., Brown, B.A., Palmenberg, A.C., 2014. Binding interactions between the encephalomyocarditis virus leader and protein 2A. J.Virol. 88, 13503–13509.
Pollard, V.W., Michael, W.M., Nakielny, S., Siomi, M.C., Wang, F., Dreyfuss, G., 1996. A novel receptor-mediated nuclear protein import pathway. Cell 86, 985–994.
Porter, F.W., Palmenberg, A.C., 2009. Leader-induced phosphorylation of nucleoporins correlates with nuclear trafficking inhibition of cardioviruses. J.Virol. 83, 1941–1951.
Porter, F.W., Bochkov, Y.A., Albee, A.J., Wiese, C., Palmenberg, A.C., 2006. A picornavirus protein interacts with Ran-GTPase and disrupts nucleocytoplasmic transport. Proc. Natl. Acad. Sci. USA 103, 12417–12422.
Porter, F.W., Brown, B., Palmenberg, A., 2010. Nucleoporin phosphorylation triggered by the encephalomyocarditis virus leader protein is mediated by mitogen-activated protein kinases. J.Virol. 84, 12538–12548.
Ricour, C., Borghese, F., Sorgeloos, F., Hato, S.V., van Kuppeveld, F.J., Michiels, T., 2009. Random mutagenesis defines a domain of Theiler's virus leader protein that is essential for antagonism of nucleocytoplasmic trafficking and cytokine gene expression. J.Virol. 83, 11223–11232.
Ricour, C., Delhaye, S., Hato, S.V., Olenyik, T.D., Michel, B., van Kuppeveld, F.J., Gustin, K.E., Michiels, T., 2009. Inhibition of mRNA export and dimerization of interferon regulatory factor 3 by Theiler's virus leader protein. J.Gen.Virol. 90, 177–186.

Ryan, K.J., Wente, S.R., 2000. The nuclear pore complex: a protein machine bridging the nucleus and cytoplasm. Curr. Opin. Cell Biol. 12, 361–371.
Sheehy, A.M., Gaddis, N.C., Choi, J.D., Malim, M.H., 2002. Isolation of a human gene that inhibits HIV-1 infection as is supressed by the viral Vif protein. Nature 418, 646–650.
Terry, L.J., Wente, S.R., 2009. Flexible gates: dynamic topologies and functions for FG nucleoporins in nucleocytoplasmic transport. Eukaryot. Cell 8, 1814–1827.
Watters, K., Palmenberg, A., 2011. Differential processing of nuclear pore complex proteins by rhinovirus 2A proteases from different species and serotypes. J. Virol. 85, 10874–10883.
Watters, K., Inankur, B., Warrick, J., Sherer, N.M., Yin, J., Palmenberg, A., 2015. Differential disruption of nucleocytoplasmic trafficking by rhinovirus 2A proteases. Mol. Biol. Cell, under review.
Wen, W., Meinkotht, J.L., Tsein, R.Y., Taylor, S.S., 1995. Identification of a signal for rapid export of proteins from the nucleus. Cell 82, 463–473.
Yaseen, N.R., Blobel, G., 1997. Cloning and characterization of human karyopherin β3. Proc. Natl. Acad. Sci. USA 94, 4451–4456.
Zehorai, E., Yao, Z., Plotnikov, A., Seger, R., 2010. The subcellular localiation of MEK and ERK—a novel translocation signal (NTS) paves a way to the nucleus. Mol. Cell Endocrinol. 314, 213–220.